# Optical Gradient Forces of Strongly Localized Fields

Tsvi Tlusty,[1] Amit Meller,[2] and Roy Bar-Ziv[3]
[1]*Department of Materials and Interfaces, The Weizmann Institute of Science, Rehovot, 76100, Israel*
[2]*Rowland Institute for Science, 100 Edwin Land Boulevard, Cambridge, Massachusetts 02142*
*and Center for Advanced Biotechnology, Boston University, Boston, Massachusetts 02215*
[3]*Center for Studies in Physics and Biology, The Rockefeller University, 1230 York Avenue, New York, New York 10021*
(Received 23 April 1998)

We present a new approach for determining optical gradient forces applied by strongly focused laser beams on dielectric particles. We show that when the electromagnetic field is focused to a diffraction limited spot a dipole approximation is valid for any particle size. We derive intuitive predictions for force-displacement curves, maximal trapping forces, and force constants. The theory fits well with recent measurements of particles trapped by laser tweezers. We also discuss effects of radiation pressure and gravity. [S0031-9007(98)06883-5]

PACS numbers: 87.64.–t, 05.40.+j, 42.25.Fx

The technique of optical tweezers has opened new experimental horizons in the biophysical and colloidal realm. Since the pioneering work of Ashkin [1–3], who first introduced the use of optical gradient forces, researchers have found diverse applications of trapping and manipulating single particles such as dielectric spheres and cellular organelles. Recent work with laser tweezers has allowed quantitative measurements of piconewton forces and nanometer displacements such as those produced by the action of single molecular motors. In addition, laser tweezers are widely used to measure mechanical elastic properties of cellular components such as DNA strands, molecular filaments, and membranes [4–6]. These experimental advances require an understanding and determination of optical gradient forces in a predictive and tractable manner. Theoretical calculations to date that predict the force acting on a general particle are strictly applicable to either small particles (electromagnetic theory) or very large particles (ray optics calculations) [7,8]. In the intermediate regime (typically $1-10\ \mu$m), which is often the most interesting one, both theories are incompatible with experimental results [4].

In previous work on optical gradient forces two main approaches have been applied, an electromagnetic (EM) approach and a ray optics (RO) approximation. In the EM approach one calculates the Maxwell stress tensor to obtain the force acting on the particle where the EM fields are computed by plane wave Fourier decomposition of the focused beam [7]. For particles of size $R$ much smaller than the wavelength of the light beam, $\lambda$, the EM approach reduces to a dipole approximation where the particle interacts with the EM field only as an electric dipole (Rayleigh theory). To compute the interaction with a focused beam in the intermediate regime, where $R$ is comparable to $\lambda$ and interference effects are relevant, one needs to sum over many Fourier components and solve the general Mie problem for each plane wave component [7]. This makes the calculation practically intractable and difficult to compare with experiment, yielding predictions of forces which are typically weaker by a factor of 3–5 compared to experimental results [4].

For very large particles, $R \gg \lambda$, and relatively small optical gradients, one can reduce EM theory to geometrical ray optics approximation. These calculations are based on a vectorial summation of the contributions of single rays, which are reflected and refracted by the particle [8] and predict a force which is independent of the particle size, with an acceptable agreement with experimental results for $R \geq 10\lambda$.

In this Letter we present a new approach for calculating the interaction of a dielectric particle with a highly inhomogeneous beam. Rather than decomposing the fields into Fourier modes we use the strong localization of the fields as a starting point for a simplified real space calculation. In the case where the beam is highly localized, the phase of the EM fields does not vary appreciably over the diffraction limited spot $\omega$. Hence, the main contribution to the interaction arises from the steep variations in the amplitude of the fields and not from interference effects which implies a dipole approximation. In the EM approach, where one decomposes the fields into plane waves, the interaction is determined by a sum over the entire volume of the particle. In contrast, for a highly focused beam the relevant length scale for interaction is the spot size $\omega$ and not $R$. This strongly reduces interference effects and renders this approach applicable to particles of *any size*.

Applying the dipole approximation to a spherical particle we derive intuitive predictions for the optical gradient interaction including important measurable quantities such as the three-dimensional force constants, force-displacement curves, and maximal trapping forces. These results agree with published experimental data obtained by various techniques such as laser tweezers interferometry [9], force feedback trapping [5], and localized dynamic light scattering [10,11].

*Electrodynamic continuum theory.*—The force due to the interaction of the electromagnetic field with a particle is given by the integral of the Maxwell stress tensor

 0031-9007/98/81(8)/1738(4)$15.00 

$\sigma_{ik}$, on its surface: $F_i = \oint \sigma_{ik} dS_k$, where $\sigma_{ik} = \frac{1}{4\pi} \times [\varepsilon E_i E_k + B_i B_k - \frac{1}{2}(\varepsilon E_i E_i + B_i B_i)\delta_{ik}]$. For a highly focused beam the main contribution to the interaction comes from the electrostatic part of the stress tensor, $\frac{\varepsilon}{4\pi}[E_i E_k - \frac{1}{2} E_i E_i \delta_{ik}]$. In this case, one can express the force as the change in the dipole interaction, $-\frac{1}{2}\int E_0 \cdot P\, dV$, with respect to the change of the particle's coordinates, where $E_0$ is the unperturbed electric field and $P$ is the dipole density [12]. For an isotropic material with a linear response the dipole density relates to the field by $P = \chi E$, where $\chi = \frac{\varepsilon - 1}{4\pi}$ is the dielectric susceptibility. For dielectrics which are not strongly polarized ($\chi \ll 1$) $E$ can be replaced by the unperturbed field and thus $P = \chi E_0$. This reduces the expression for the dipole interaction energy of the particle, $W$, to the integral of the unperturbed energy density, $I = \varepsilon_0 E_0^2/8\pi$, over the volume of the particle:

$$W = -\alpha \int I\, dV\,. \tag{1}$$

$\alpha = \frac{\varepsilon_p}{\varepsilon_0} - 1$ accounts for the relative difference of the dielectric constants of the particle, $\varepsilon_p$, and the surrounding medium, $\varepsilon_0$. Then, the optical gradient force is simply given by the change of $W$ in response to a change of the particle's coordinates.

*Results.*—To compare our approach with experimental measurements on laser trapping of dielectric particles, we calculate explicitly the force exerted on a spherical particle in a potential formed by optical tweezers. We approximate the localized electromagnetic fields near the focal point by a three-dimensional Gaussian beam of axial symmetry, whose energy density is

$$I(\rho, z) = I_0 \exp\left(-\frac{\rho^2}{2\omega^2} - \frac{z^2}{2\omega^2\epsilon^2}\right), \tag{2}$$

where $\omega$ and $\omega\epsilon$ are the dimensions of the beam waist in the transverse and axial directions, respectively, and the eccentricity is $\epsilon$. The frame of reference is defined by the geometrical focus of the beam, $\rho = z = 0$. The polarization interaction forms a potential well with a restoring force which tends to pull back the particle to its equilibrium position, at the center of the beam ($r = 0$). Because of the spherical symmetry of the particle the electrostatic energy, $W$, depends only on the position of its center of mass, $\vec{r}$.

To demonstrate the main physical principles we first consider the case of an isotropic potential well, $\epsilon = 1$. Taking the gradient of the dipole energy, Eq. (1), inside the Gaussian beam, Eq. (2), we obtain a central restoring force,

$$\begin{aligned} F(r) &= \partial_r W(r) \\ &= \alpha I_0 \omega^2 4\pi e^{-(a^2+u^2)/2}[au\cosh(au) - \sinh(au)], \end{aligned} \tag{3}$$

where $a = R/\omega$ and $u = r/\omega$ are the normalized radius and coordinate, respectively.

For small particles $R \ll \omega$, Eq. (3) reduces to $F \simeq V\alpha\nabla I = \alpha I_0 \omega^2 \frac{4\pi}{3} a^3 u e^{-u^2/2}$, which is the product of the local gradient of the beam intensity and the particle volume. Near the equilibrium position, $r \approx 0$, the restoring force is harmonic and increases to its peak value at the position of maximal gradient, $r = \omega$, where the force is $F_m = \alpha I_0 \omega^2 (4\pi/3\sqrt{e}) a^3$. This scenario changes drastically as the particles become much larger than the beam waist, $R \gg \omega$. In this case the force results mainly from the movement of the particle boundaries in the inhomogeneous intensity. When the particle is located around the center, $r \ll R$, its boundaries feel the tail of the decaying Gaussian intensity, $I(R) \sim e^{-(1/2)a^2}$, resulting in a weak force. The force becomes significant only for $r \simeq R$, when part of the boundary is close to the center of the beam. The restoring force for this case is well approximated by $F \simeq \alpha I_0 \omega^2 2\pi (\frac{a}{u}) e^{-(1/2)(u-a)^2}$ which exhibits a sharp peak of width $\Delta r = \omega$ and amplitude $F_m \simeq \alpha I_0 \omega^2 2\pi$ located at $r = R$, thus defining an approximately cylindrical potential well of diameter $2R$ and depth $\Delta U \simeq (2\pi)^{3/2} \alpha I_0 \omega^3 \sim F_m \Delta r$. In the intermediate region the maximal force crosses over continuously from the $R^3$ scaling for small particles to be size independent for very large particles. We note that this asymptotic result, $F_m \simeq \alpha I_0 \omega^2 2\pi$, is insensitive to the specific geometry of the particle; namely, it remains the same for any particle (not only spherical) whose radius of curvature is much larger than the beam width.

In most practical situations, focused beams are not isotropic having eccentricity, $\epsilon$, of roughly 3 or even more. In these cases the energy integral [Eq. (1)], used to calculate the isotropic force [Eq. (3)] leads to cumbersome numerics. However, to simplify the numerical integration one can approximate our spherical trapped particle by a cube of the same volume. The resulting force curve for a general eccentricity, $\epsilon$, is

$$\frac{F_\rho(\rho)}{\alpha I_0 \omega^2} = A(\epsilon) e^{-(1/2)u^2} \sinh(a_c u)\,. \tag{4}$$

Note that all the anisotropy effects are embedded in a prefactor, $A(\epsilon)$,

$$A(\epsilon) = 4\pi\epsilon \operatorname{erf}\left(\frac{b_c}{\sqrt{2}}\right) \operatorname{erf}\left(\frac{b_c}{\sqrt{2}\,\epsilon}\right) e^{-(1/2)a_c^2}, \tag{5}$$

where $a_c = b_c = \frac{R}{\omega}(\frac{\pi}{6})^{1/3}$, and $u = \frac{\rho}{\omega}$. A similar expression can be found for the axial direction [13].

Figure 1 shows a force-displacement curve calculated from Eq. (4). The theoretical curve is superimposed on the data extracted from Fig. 5 in Simmons *et al.* [5], with the experimental values, $\omega = 0.29\ \mu$m, $R = 0.5\ \mu$m, and $\epsilon = 3$. The curve exhibits the linear Hookian response for small displacements in the vicinity of the center of the beam. It also shows the maximal trapping force and the decay at large displacements. At large displacements the theory overestimates the observed force possibly due to the cutoff of the actual beam at long distances.

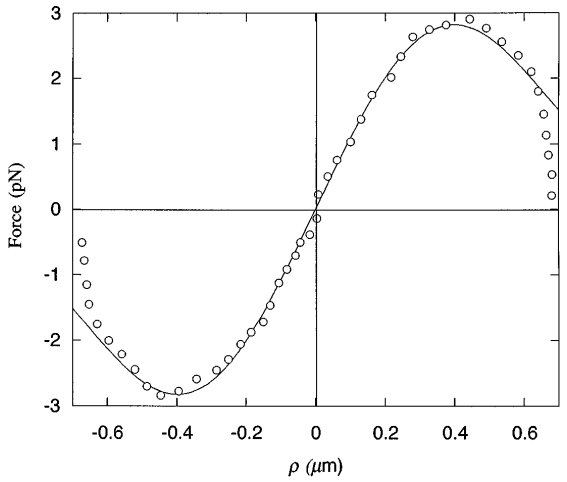


FIG. 1. Force-displacement curve for a spherical particle. Circles are experimental data extracted from Ref. [5], for particle of size $R = 0.5\ \mu$m, lateral beam width $\omega = 0.29$, and eccentricity $\epsilon = 3$. The theoretical curve (solid) is taken from Eq. (4) using the experimental parameters. Note that the force reaches its maximum value for $\omega \leq \rho \leq R$ and vanishes for longer distances as the particle exits the beam. The data deviate from the fit for $\rho > 0.6\ \mu$m due to experimental cutoff.

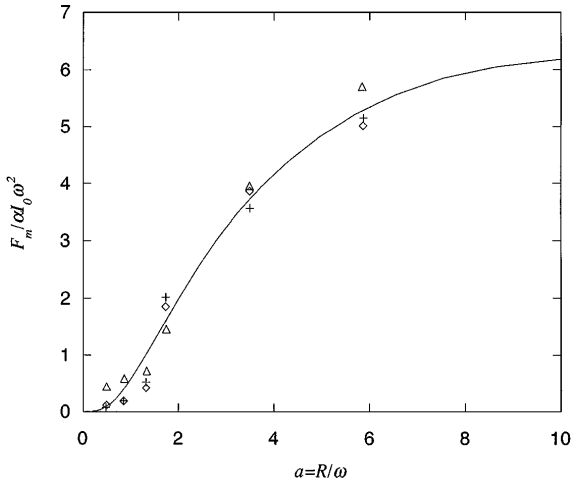


FIG. 2. Normalized maximal force, $F/\alpha I_0\omega^2$, as a function of the particle's normalized size, $a = R/\omega$. The theoretical curve (solid) was obtained by maximizing the force-displacement curve, Eq. (4) (see text), and using the experimental parameters $\omega = 0.29\ \mu$m and $\epsilon = 3$ as in Fig. 1. Crosses, diamonds, and triangles are data points extracted from Fig. 10 of Ref. [5] for laser intensities of 100, 50, and 13 mW, respectively.

In order to check the validity of the approximation leading to Eq. (4), we compared the results of this equation for the isotropic case, $\epsilon = 1$, with the exact formula for a sphere, Eq. (3), and obtained a maximal force which differs by less than 5%. We note that for very large particles ($a \geq 4$) an additional correction improves the agreement [14].

Going back to Fig. 1 we see that the force exhibits a maximum at a distance comparable with the particle size. In Fig. 2 we plot the maximal trapping force together with the maximal forces extracted from Fig. 10 of Ref. [5], as a function of particle size. The location of the maximum, $u_m$, is obtained by differentiating the force [Eq. (4)] and solving the resulting transcendental equation, $\tanh(a_c u_m) = a_c/u_m$. The consequent maximal force obtained this way shows the same qualitative behavior discussed for the isotropic case, Eq. (3). In particular, for small particles we recovered the $R^3$ dependence of the force and an asymptotic plateau at large particles. Using the same parameters as in Fig. 1 we find a remarkable agreement with the experimental data over the entire range of particle size.

In the vicinity of the equilibrium position, $\vec{r} = 0$, the well is approximately harmonic. For this region it is useful to define the force constant given by the curvature of the potential. For the isotropic case we obtain from Eq. (3) a force constant

$$\frac{\kappa_I}{\alpha I_0 \omega} = \frac{4\pi}{3} a^3 e^{-a^2/2}, \tag{6}$$

which is proportional to the volume for small particles and decays exponentially for large ones. For the anisotropic case $\kappa_I$ is split into two different values, $\kappa_\rho$ and $\kappa_z$, for transverse and longitudinal directions, respectively. As opposed to the force-displacement curve this can be calculated analytically for a sphere, yielding

$$\frac{\kappa_z}{\alpha I_0 \omega} = \frac{4\pi}{\xi^3}\left[\sqrt{\frac{\pi}{2}}\,\mathrm{erf}(\xi a/\sqrt{2}) - \xi a e^{-a^2/2}\right], \tag{7}$$

$$\frac{\kappa_\rho}{\alpha I_0 \omega} = \frac{2\pi\epsilon^2}{\xi^3}\left[\sqrt{\frac{\pi}{2}}[(\xi a)^2 - 1]e^{-a^2/2\epsilon^2} \times \mathrm{erf}(\xi a/\sqrt{2}) + \xi a e^{-a^2/2}\right], \tag{8}$$

where $\xi = \sqrt{1 - \epsilon^2}$ is the anisotropy.

In Fig. 3 we plotted the theoretical $\kappa_\rho$ along with data extracted from various experiments: (1) Laser tweezers interferometry [9], (2) force feedback trapping [5], and (3) localized dynamic light scattering [10,11]. We rescaled the particles' radii measured in the different experiments with their corresponding beam waists. The theoretical curve (solid line) is plotted for an eccentricity, $\epsilon = 3$. We observe a maximal force constant around $R/\omega \approx 2$, which corresponds to the location of the maximal gradient of the force curve (Fig. 2). The agreement with the various data is remarkable for the region of small particles around the steep peak, while a large inconsistency is found for the largest particles measured. We suggest that this deviation is mostly due to the dominant contributions from anharmonic terms to the measured spring constant and possible effects of gravity and radiation pressure as discussed in the following.

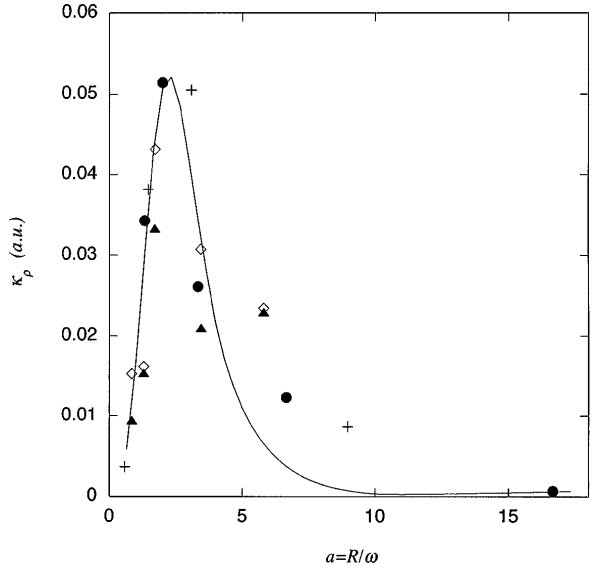


FIG. 3. The transverse force constant $\kappa_\rho$ versus normalized particle size $a = R/\omega$ for the eccentricity $\epsilon = 3$ calculated from Eq. (8). The theoretical prediction is verified by overlaying experimental data from several references using different experimental techniques: Empty diamonds and solid triangles are data taken from Ref. [5] for two laser intensities 52 and 13 mW, correspondingly. Crosses are data taken from Ref. [9], and solid circles are our data measured by localized dynamic light scattering (unpublished).

*Radiation pressure and gravity.*—In the preceding discussion we neglected the effect of radiation pressure which tends to push the particle forward along the beam axis. Our simple approach naturally explains why radiation pressure cannot overcome the gradient force and destabilize the particle unless the beam waist is large enough. For small particles $R \ll \lambda$, the radiation pressure force is proportional to the Rayleigh dipole scattering cross section [12], and thus scales like $F_{\rm rad} \sim I_0 \lambda^2 \alpha^2 (\frac{R}{\lambda})^6$. We recall that the maximal gradient force for small particles $F_m \sim I_0 \omega^2 \alpha (\frac{R}{\omega})^3$ and hence $F_{\rm rad}/F_m \sim \alpha \omega R^3/\lambda^4$. For a diffraction limited spot, $\omega \approx \lambda$, this ratio is just $\alpha (R/\omega)^3 \ll 1$, and thus the particle is strongly trapped. Escape is possible only for very wide beam waists, $\omega \geq \lambda^4/R^3\alpha$. However, small particles may escape due to thermal fluctuations which sets a lower bound on the particle size by comparing the trapping interaction with the thermal energy, $R_{\rm c} \sim (k_B T/\alpha I_0)^{1/3}$. For large particles radiation pressure scales like $F_{\rm rad} \simeq 2\pi\alpha^2 I_0 \omega^2$, while $F_m \simeq 2\pi\alpha I_0 \omega^2$ and hence $F_{\rm rad}/F_m \simeq \alpha$. Consequently, almost transparent particles ($\alpha \ll 1$) are strongly trapped $F_{\rm rad} \ll F_m$.

Finally, we consider the effects of gravitation. The gravitational force is $F_g = \frac{4\pi}{3} R^3 \Delta\rho g$, where $\Delta\rho$ is the mass density difference of the particle and its neighborhood. Hence, by comparing this to the maximal gradient force we find that gravitational effects will be relevant for large particles at $R \geq (\alpha I_0 \omega^2/\Delta\rho g)^{1/3}$ and for small particles at $\Delta\rho g \omega \geq \alpha I_0$. In this region we expect the force constant in the longitudinal direction to vanish when the gravitational force is equal to the optical gradient force. Such behavior was indeed observed in localized dynamic light scattering experiments of large trapped silica beads where we measured weak force constants and escape [11].

In summary, we presented a simple intuitive approach to calculate gradient forces of highly localized fields on dielectric particles. The formalism predicts quantitative results which are in good agreement with experimental data measured by laser trapping. We hope this approach will be useful for quantitative interpretation of force measurement experiments.

We thank S. A. Safran, E. Moses, and J. Stavans for illuminating discussions and for a fruitful collaboration.

[1] A. Ashkin, Phys. Rev. Lett. **24**, 156–159 (1970).
[2] A. Ashkin, Science **210**, 1081–1088 (1980).
[3] A. Ashkin, J. M. Dziedzic, and T. Yamane, Nature (London) **330**, 769–771 (1987).
[4] K. Svoboda and S. M. Block, Annu. Rev. Biophys. Biomol. Struct. **23**, 247–285 (1994).
[5] R. M. Simmons, J. T. Finer, S. Chu, and J. A. Spudich, Biophys. J. **70**, 1813–1822 (1996).
[6] A. Ashkin, Proc. Natl. Acad. Sci. U.S.A. **94**, 4853–4860 (1997); A. Ashkin, Methods Cell Biol. **55**, 1–27 (1998).
[7] M. Kerker, *The Scattering of Light and other Electromagnetic Radiation* (Academic, New York, 1969).
[8] A. Ashkin, Biophys. J. **61**, 569–582 (1992).
[9] L. P. Ghislain, N. A. Switz, and W. W. Webb, Rev. Sci. Instrum. **65**, 2762–2768 (1994).
[10] R. Bar-Ziv, A. Meller, T. Tlusty, E. Moses, J. Stavans, and S. A. Safran, Phys. Rev. Lett. **78**, 154–157 (1997).
[11] A. Meller, R. Bar-Ziv, T. Tlusty, E. Moses, J. Stavans, and S. A. Safran, Biophys. J. **74**, 1541–1548 (1998).
[12] L. D. Landau and E. M. Lifshitz, *Electrodynamics of Continuous Media* (Pergamon, New York, 1982).
[13] Similarly, we obtain the same spatial dependence for the axial force, $F_z(z)/\alpha I_0 \omega^2 = A_z(\epsilon) \sinh(a_c u_z) e^{-(1/2)u_z^2}$, where the coordinate is $u_z = z/\omega\epsilon$ and the prefactor $A_z(\epsilon) = 4\pi\,\mathrm{erf}(b_c/\sqrt{2})^2 e^{-(1/2)(a_c/\epsilon)^2}$.
[14] To improve the compatibility with the exact calculation for very large spheres we integrate instead over a rectangular box having the same volume yielding the same expression (4) but with $b_c = \sqrt{\pi/6}\, a_c = \frac{R}{\omega}$.